environments

MDPI

Article

Level of Pollution and Health Risks from Heavy Metals in Volcanic Ash and Street Dust in the City of Puebla, Mexico

Miguel Santoyo-Martínez [1,*], Francisco Bautista [2], Avto Goguitchaichvili [3], Miguel Á. Valera-Pérez [1], Patricia Quintana [4] and María G. Tenorio-Arvide [1,*]

[1] Laboratorio de Geoquímica Ambiental, Centro de Investigación en Ciencias Agrícolas (CICA), Instituto de Ciencias (ICUAP), Benemérita Universidad Autónoma de Puebla (BUAP), Puebla 72000, Puebla, Mexico
[2] Laboratorio Universitario de Geofísica Ambiental (LUGA), Centro de Investigaciones en Geografía Ambiental (CIGA), Universidad Nacional Autónoma de México (UNAM), Morelia 58190, Michoacán, Mexico
[3] Laboratorio Universitario de Geofísica Ambiental (LUGA), Instituto de Geofísica, Universidad Nacional Autónoma de Mexico (UNAM), Morelia 58190, Michoacán, Mexico
[4] Departamento de Física Aplicada, Laboratorio Nacional de Nano y Biomateriales (LANNBIO), Centro de Investigación y de Estudios Avanzados (CINVESTAV), Merida 97310, Yucatán, Mexico
* Correspondence: miguel.santoyom@correo.buap.mx (M.S.-M.); tenorio.arvide@correo.buap.mx (M.G.T.-A.); Tel.: +52-222295500 (ext. 7043) (M.S.-M. & M.G.T.-A.)

Abstract

Heavy metals in urban dust, derived from anthropogenic activities and natural sources, are considered potentially toxic elements for human health. The city of Puebla, located in Central Mexico, is one of the ten largest metropolitan cities in Mexico. Near this city is the Popocatépetl volcano, which contributes heavy metals through the emission of ash. The objectives of this study were to evaluate heavy metal contamination in urban dust and volcanic ash from the city of Puebla, and to determine the associated human health risks. Heavy metals were analyzed using an XRF spectrometer. The level of contamination was established according to the contamination factor, the geoaccumulation index and the contaminant load index. Furthermore, non-carcinogenic risk indices (HIs) were calculated to evaluate the health risk. The results revealed the presence of 18 elements (Ca, Cr, Cu, Fe, K, Mn, Nb, Ni, Pb, Rb, Sb, Sn, Sr, Ti, Y, V, Zn and Zr), with the highest concentrations found for most in urban dust samples, while Rb, Ca and K showed higher concentrations in ash samples. High levels of Sb and Sn contamination were found in 90 to 100% of the dust and ash samples, while Cr, Cu, Ni, Pb and Zn showed considerable levels of contamination in 60 to 90% of the samples. According to the US EPA thresholds, the health risk assessment indicated safe levels (HI < 0.25) for Cu, Fe, Mn, Ni, Pb, Sn, V and Zn in the urban dust and volcanic ash samples, while some of the samples exceeded the safety threshold (HI > 1) for Cr and Sb with respect to the child population in the city of Puebla. These results must be taken into consideration by environmental and government authorities, and the degree of pollution should be reduced accordingly.

Keywords: heavy metals; street dust; volcanic ash; environmental pollution; health risk; city of Puebla

Check for updates

Academic Editor: Gianniantonio Petruzzelli

Received: 23 December 2025
Revised: 27 February 2026
Accepted: 3 March 2026
Published: 10 March 2026

Copyright: © 2026 by the authors. Licensee MDPI, Basel, Switzerland. This article is an open access article distributed under the terms and conditions of the Creative Commons Attribution (CC BY) license.

1. Introduction

Heavy metal (HM) pollution levels have increased in recent years [1]. Anthropogenic activities are the main source of HM emissions [2], including industrial processes, vehicular emissions and wear of automotive parts, among others [3–5]. On the other hand, although

less recurrent, forest fires and volcanic eruptions have been identified as natural sources of HM pollution [6–11].

HMs dispersed in the environment can adhere to soil particles, where they are deposited on the street surface in urban settings [12–14]. Particles smaller than <10 µm [15–17] can enter the body through inhalation, ingestion and dermal contact [18,19] and, depending on the type of element, susceptibility and exposure time, can pose a threat to human health [20,21].

HMs include non-essential elements that do not fulfill a metabolic function in humans, such as arsenic (As), cadmium (Cd), mercury (Hg) and lead (Pb), which are toxic even at low concentrations [20] due to their capacity to accumulate in different tissues and cause damage [22]. For example, they can affect the internal organs [23], cause cardiovascular and respiratory diseases [20], and induce DNA damage that promotes the development of cancers [24]. Elements that have been commonly reported in street dust include As, Cd, copper (Cu), Chromium (Cr), manganese (Mn), nickel (Ni), Pb and zinc (Zn) [14,25–30].

The study of HM pollution in cities entails particular considerations regarding the potential natural sources (e.g., rocks, landforms, soil, volcanoes, winds, vegetation) [31] and anthropogenic sources (e.g., time and type of construction materials for urban infrastructure, type of companies and industries, type of fuels used) [32,33]. These factors, together with the urban form and its diversity of activities, make each city a particular case, leading to differences in the concentrations of elements between cities [27,29,34–36].

Studies focused on HMs in street dust have been documented in various parts of the world [30,37–40]. In Mexico, such studies have been performed in various states, including Torreón, Coahuila [41]; Hermosillo, Sonora [42]; the Monterrey Metropolitan Area [43]; Gómez Palacio, Durango [29]; Mérida, Yucatán [34]; and Mexico City [36]. The previously mentioned studies suggested the need to conduct further research in different cities, which would allow us to better understand the dynamics of HM in different cities, their pollution levels, and the possible sources of these elements. This information is relevant for decision-making and starting the search for potential solutions to the complex environmental and health problems that the human population currently faces.

This study was carried out in the capital of the state of Puebla—the city of Puebla—which is one of the most populated cities in Mexico, with 1,692,181 inhabitants [44]. Located in the center of the country, the city of Puebla has a high level of pollution derived from industrial activities focused on automotive, food and textiles, in addition to having a high density of urban traffic with approximately 578,200 vehicles.

The Popocatépetl volcano is located 50 km from the city of Puebla. It is part of the Trans-Mexican Volcanic Belt and is a stratovolcano covering more than 500 km^2, with a crater 900 m wide and an altitude of 5452 meters above sea level; Strombolian and Vulcanian activity have been reported in some events. After 70 years of calm, its activity resumed in December 1994 and has remained constant to date, emitting incandescent material and volcanic ash, which falls on the city of Puebla [45,46]. However, the level of HM pollution and the possible human health risks in the city remain unknown. Based on the above, the objective of this study is to determine the concentrations, pollution levels and human health risks associated with heavy metals in volcanic ash and street dust from the city of Puebla.

2. Materials and Methods

2.1. Study Site

Puebla's capital is geographically located at 19°03′05″ N and 98°13′04″ W, in the central part of Mexico, with a population density of 64 inhabitants/km^2 [44]. At an altitude of 2140 meters above sea level, it has a temperate climate, with an average annual

precipitation of 961 mm and an average annual temperature of 17.2 °C. The vegetation is characterized as temperate forest, grasslands and induced shrublands [47].

2.2. Sampling of Dust in the Streets and Volcanic Ash of the City of Puebla

Dust samples were collected from 60 street locations with a systematic and homogeneous distribution (see Figure 1). In February 2023, 2 m^2 sidewalk areas were selected, manually removing stones, branches and leaves. Subsequently, the area was swept with a brush, forming four piles of dust. Using a plastic dustpan, these piles were collected in polyethylene bags previously labeled with the site number and geographic location data. Volcanic ash was collected from 40 sites after it fell in May 2023. It was collected with a brush, taking the top part of the ash accumulated on the ground while avoiding dust already present on the ground.

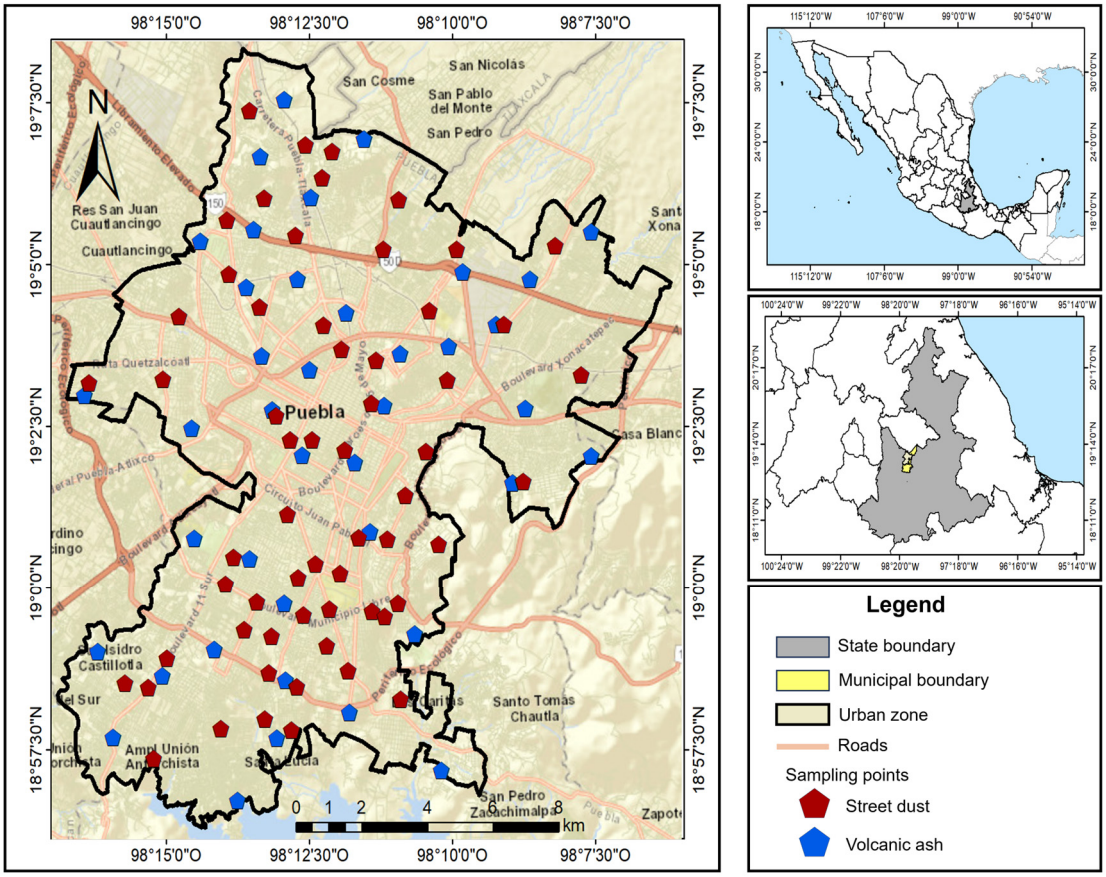


Figure 1. Location of the urban dust and volcanic ash sampling sites.

2.3. Processing and Analysis of Heavy Metals

Samples of volcanic ash (40) and dust (60) were sieved using a mesh with a 53 µm aperture to separate 3 g of sample, which was collected in a Teflon cup covered on the bottom with a 3.6 µm thick Mylar (polyester) film. Elemental analysis was performed using a Genius 7000 XRF portable spectrometer, with an estimated measurement time of 180 s per sample. The measurements of each sample were carried out in triplicate, for a total of 300 measurements. A lateritic soil sample was used as a control with a set of eight internationally certified geochemical reference materials for rocks and soils, with identification code IGLs-1 [48].

2.4. Mineralogy and Morphology of Street Dust Particles and Volcanic Ash

Representative samples of urban dust and volcanic ash were selected for X-ray diffraction (XRD) analysis. According to [49], a Bruker D-8 Advance diffractometer with monochromatic Cu Kα (λ = 1.5418 Å) radiation, a passage time of 0.5 s, and a size of 0.02 degrees, with analyses performed at 40 kV and 30 mA. For analysis, the powders were placed on a silicon sample holder coated with appropriate vacuum grease for XRD.

The shape and size of dust and ash particles were determined for representative samples via photomicrographs captured with a Philips ESEM XL30 scanning electron microscope coupled to EDAX GENESIS with a SiLi detector, 10 L, 204Bt (SEM-EDS) [34,49].

2.5. Analysis of Pollution Levels

Three parameters were calculated to determine the contamination levels for the HMs detected in samples: (1) the contamination factor (CF) [50], (2) the geoaccumulation index (Igeo) [51] and (3) the pollution load index (PLI) [52]. The latter uses the average CF of the eight highest elements (Equations (1)–(3)). Table S1 presents the interpretation of the Igeo, CF and PLI results.

$$CF = C_n / B_n \quad (1)$$

$$Igeo = Log_2\left(\frac{C_n}{1.5B_n}\right) \quad (2)$$

$$PLI = \sqrt[n]{CF1 * CF2 * \ldots .. * \ CFn} \quad (3)$$

Here, C_n is the concentration of the nth metal in the sample analyzed and B_n is the background value of the same metal (in this case, the B_n values correspond to global soil background values) [53].

2.6. Assessment of Risks to Human Health from Exposure to Heavy Metals in Dust and Volcanic Ash

To estimate the human health risks due to exposure to HMs in volcanic ash and dust, following the methodology of the United States Environmental Protection Agency (US EPA) [54], values were estimated for the following routes of exposure: ingestion (EDI_{ing}), inhalation (EDI_{inh}) and dermal contact (EDI_{der}) (Equations (4)–(6)).

$$EDI_{ing} = \frac{C \times IngR \times ED \times CF}{BW \times AT} \quad (4)$$

$$EDI_{inh} = \frac{C \times InhR \times ED \times EF}{PEF \times BW \times AT} \quad (5)$$

$$EDI_{dermal} = \frac{C \times SA \times AF \times ABS \times EF \times ED \times CF}{BW \times AT} \quad (6)$$

Following the US EPA methodology [54], the risk indices for each exposure route—namely, ingestion, inhalation, and dermal contact ($HQ_{ing/inh/derm}$, respectively)—were obtained by dividing the EDI by the reference dose (RfD) for each metal, as shown in Equation (7). The hazard index (HI) was obtained by summing all of the individual hazard quotients (HQs) for each metal, as shown in Equation (8). If the HI is >1, there is an increased probability of non-cancer health risks in the exposed population; meanwhile, if its value is <1, the opposite would be expected [54]. For this study, exposure factors established for the reference populations were used (Table S2) (references [55–59] are cited in the Supplementary Material).

$$HQ_{ing/inh/derm} = \frac{EDI_{ing/inh/derm}}{RfD} \quad (7)$$

$$HI = \sum HQ \tag{8}$$

For carcinogenic elements, the incremental lifetime cancer risk (ILCR) was determined using the lifetime average daily dose (LADD) and slope factors for each exposure route (CSF) (Table S3). In particular, it was calculated for Cr, Ni and Pb, as these were the carcinogenic elements found to be present in the tested samples (Equations (9) and (10)).

$$\text{LADD} = \frac{C}{\text{PEF} \times \text{ATcan}} \times \left(\frac{\text{CRchild} \times \text{EFchild} \times \text{EDchild}}{\text{BWchild}} + \frac{\text{CRadult} \times \text{EFadult} \times \text{EDadult}}{\text{BWadult}} \right) \tag{9}$$

$$\text{ILCR} = \text{LADD} \times \text{CDF} \tag{10}$$

The data obtained were statistically analyzed using the Origin 2023 package [60]. A nonparametric test was performed, as the data did not present a normal distribution according to the Shapiro–Wilk test result. A Mann–Whitney U test was conducted to compare the concentrations of HMs in urban dust and volcanic ash, and Spearman's evaluation analysis was performed to determine the relationships between the elements detected in the urban dust samples and the volcanic ash [61].

3. Results and Discussion

3.1. Elements Concentration

Eighteen elements were detected in the tested street dust and volcanic ash samples: calcium (Ca), Cr, Cu, iron (Fe), potassium (K), Mn, niobium (Nb), Ni, Pb, rubidium (Rb), antimony (Sb), tin (Sn), strontium (Sr), titanium (Ti), yttrium (Y), vanadium (V), Zn, and zirconium (Zr). The data did not present a Gaussian distribution, according to the Shapiro–Wilk test result.

The concentrations of the elements detected in dust samples showed the following pattern: Ca > Fe > K > Ti > Mn > Sr > Zn > Zr > Cr > Cu > V > Ni > Sb > Pb > Rb > Y > Sn > Nb. Meanwhile, the volcanic ash samples showed the following pattern: Ca > Fe > K > Ti > Mn > Sr > Zr > Zn > V > Cr > Ni > Rb > Y > Cu > Sn > Sb > Pb. Notably, Ca, Fe and K were found at higher concentrations in both dust and ash samples, which can likely be attributed to the fact that they are abundant in the Earth's crust [62]. The concentrations of Rb, Ca and K were significantly higher in the volcanic ash samples, which suggests that volcanic activities disperse these elements; relevant studies support their presence, as well as 12 of the other elements found in this study [6,63]. In contrast, the origin of Nb, Sb and Sn was considered to be related to anthropogenic activities [64,65].

The elements Cr, Cu, Fe, Mn, Nb, Ni, Pb, Sb, Sn, Ti, Y, V, Zn and Zr were found in higher concentrations in street dust samples compared to volcanic ash samples, with significant differences, while the Sr concentration did not present statistically significant differences between the dust and ash (Table 1).

The low concentrations of ash relative to dust could be due to the frequency of volcanic activity at Popocatépetl. Although it has been constantly active for 30 years, not all ash emission events affect the city of Puebla, being dependent on the intensity of the activity and the direction of the wind. However, together with Mexico City, this city reports the highest ash fall from the volcano [46].

The coefficients of variation (CVs) calculated for Cr, Cu, Pb, Sb and Zn showed high variation in the detected concentrations, which can likely be attributed to the fact that the samples that presented higher concentrations of these elements are related to various anthropogenic activities in the city, such as high vehicular flow, wear of asphalt and brake pads, and wear of paints on streets and main avenues [3].

As the volcanic ash could incorporate particles of anthropogenic origin, the concentration ratio between street dust and volcanic ash (D/A) was estimated; this method reflects

the relative intensity of urban dust versus volcanic ash [36,66]. In particular, a D/A value for a given HM greater than 1 indicates that the concentration of this metal in street dust was greater than that in volcanic ash, indicating its dominant concentration in the street dust; meanwhile, D/A < 1 indicates the origin of the element as volcanic ash. For most cases for Cr, Cu, Fe, Ni, Pb, Sb, Sn, Ti, Zn and Zr, the D/A values were greater than 1, which indicates that the concentrations of these elements were higher in street dust relative to volcanic ash. In contrast, in most cases for Ca, K, Rb, Sr, V and Y, the D/A ratio was less than 1, suggesting the possible origin of these elements as volcanic ash (see Figure 2).

Table 1. Descriptive statistics of metal element concentrations (mg/kg) in urban dust and volcanic ash in Puebla.

Metal		n	Mean	Median	Min	Max	SD	CV (%)	DL	SDT	BWS
Cr	dust	60	142	131	54	297	58	40	2	*	59.5
	ash	40	56	57	27	79	15	26			
Cu	dust	60	110	49	17	2617	339	308	0.7	*	38.9
	ash	40	24	25	16	32	5	18			
Mn	dust	60	813	813	476	1021	118	14	0.004	*	480.0
	ash	40	788	788	762	817	17	2			
Nb	dust	60	5	6	1	12	2	44	0.7	*	12.0
	ash	40	nd	nd	nd	nd	nd	nd			
Ni	dust	60	91	89	41	146	27	29	0.5	*	29.0
	ash	40	44	43	30	57	9	21			
Pb	dust	60	36	31	14	113	22	59	4	*	27.0
	ash	40	12	12	10	15	1	11			
Rb	dust	60	36	35	21	53	7	18	2	*	68.0
	ash	40	42	41	31	55	6	15			
Sb	dust	60	37	37	10	80	16	435	1	*	0.68
	ash	40	15	15	8	27	5	33			
Sn	dust	60	25	25	7	75	10	38	1	*	2.5
	ash	40	19	21	7	33	7	38			
Ti	dust	60	5331	5217	3890	7861	582	11	0.004	*	7038.0
	ash	40	38,701	3932	2359	5307	942	24			
Y	dust	60	33	33	29	36	2	5	0.5	*	23.0
	ash	40	30	29	25	35	3	10			
V	dust	60	105	104	11	189	39	37	5	*	129.0
	ash	40	79	76	10	132	32	40			
Zn	dust	60	293	224	85	1654	231	79	1.5	*	70.0
	ash	40	137	120	68	230	53	39			
Zr	dust	59	183	185	84	348	38	21	0.5	*	267.0
	ash	40	139	171	18	180	60	43			
Sr	dust	60	462	469	360	560	50	11	1	NS	175.0
	ash	40	445	439	352	533	60	14			
Ca	dust	60	59,356	58,423	40,068	88,084	8441	14	0.04	*	
	ash	40	94,128	94,655	38,670	156,753	37,261	40			
Fe	dust	60	37,800	37,743	25,760	52,132	5459	14	0.006	*	
	ash	40	32,244	32,113	27,914	35,933	2826	9			
K	dust	60	6148	6061	3976	8409	1069	17	0.05	*	
	ash	40	7205	7412	738	9747	1813	25			

nd—not detected; Min—minimum; Max—maximum; SD—standard deviation; CV—coefficient of variation; DL—detection limit (ppm); SDT—statistical differences between samples; * = $p < 0.05$; NS—not significant; BWS—world soil background.

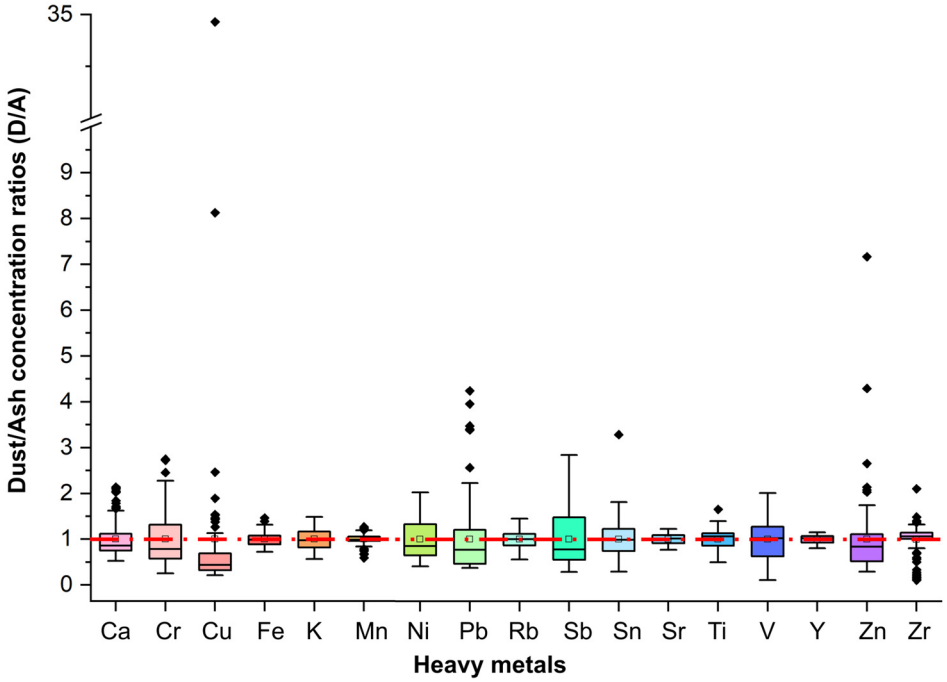


Figure 2. The dust/ash concentration ratios (D/A) of heavy metals.

The relationships between the concentrations of Cr, Cu, Fe, Ni, Pb, Sb, Sn and Zn in dust and ash, as well as their variation in the samples, suggest that these elements have been enriched by activities related to vehicular flow and the wear of the automobile parts (e.g., brakes, tires) and street asphalt [67]. Various studies have supported the anthropogenic origin of Cr, Cu, Fe, Sb, Sn, Mn, Ni, Ti and Zn.

For example, brake wear produces particles containing Cu, Fe, Zn, Ti and Sb [3,68]; Sb and Sn are present in the composition of brake pads [64,69]; tire wear releases Cu- and Zn-containing particles [68]; vehicle chassis wear releases Cu, Mn Al, Ni and Zn [70]; and Nb is found in vehicle exhaust pipes, which is released due to wear and high temperatures [65,71].

The average concentrations of V in dust samples (105 mg/kg) and volcanic ash (79 mg/kg) both exceed the maximum limit allowed in urban soils (78 mg/kg), according to the relevant Mexican standard [72]. This can be attributed to the fact that V is released into the environment via volcanic emissions, as this element is part of volcanic rocks; in addition, it is also emitted through the burning of fossil fuels (e.g., as automobile emissions). Notably, exposure to V has consequences for human health, such as triggering respiratory and cardiovascular diseases [73–75].

The HM concentrations in urban dust and volcanic ash obtained in this study were compared with those reported elsewhere (Table 2), where Cr, Cu, Mn, Ni, Pb and Zn were the most commonly evaluated elements, followed by Fe, V, Sb and Sn. In the case of Pb and Zn from urban dust, the values are generally higher than the global background values [53], followed by Cr, Cu and Sb, indicating widespread enrichment of these elements due to anthropogenic activities [3]. Meanwhile, for Mn, Ni and Sn, few studies have reported values higher than the global background values, while V did not exceed global soil values in any of the included studies (Table 2). In volcanic ash samples, concentrations of Mn and Zn were typically reported to be higher than the global background values, as was the case in this study (Table 2).

Table 2. Comparison of concentrations of ten metals in various cities around the world.

City	Cr	Cu	Fe	Mn	Ni	Pb	Sb	Sn	V	Zn	Reference
						mg/kg					
Global background	59.5	38.9	–	480	29	27	0.68	2.5	129	70	[53]
Urban dust											
Mexico, Mexico	51.4	99.7	5722.2	235.2	36.3	128.2	–	–	26.8	280.7	[27]
Dakota del Norte, USA	23.6	17.4	20,896	783.5	24.8	14.7	–	–	81.6	–	[30]
Xi'an, China	154.2	62.1	–	546.2	32.2	151.6	–	–	68.7	390.7	[37]
Toronto, Canada	145	121	–	784	36	63	4.1	11	41	419	[39]
Qom, Iran	80.2	130.0	30,768	706	40.0	367.6	6.4	–	–	708.7	[40]
Anhui, China	126.9	71.3	9868	237	19.8	2.4	2.6	2.1	31.3	244.7	[56]
Ottawa, Canada	41.8	29.5	18,000	426.4	14.6	32.9	0.4	1.19	34.2	98.7	[76]
Palermo, Italy	175.2	570.4	28,000	256.2	26.8	664.4	–	31.0	19.8	390.2	[77]
Shiraz, Iran	67.2	136.3	20,254.6	438.5	77.5	115.7	4.8	–	–	403.5	[78]
Hermosillo, Mexico	262	73	1735	528	18.7	16.6	3.1	3.5	86	12,842	[79]
Al-Karak, Jordan	51.7	57.4	–	259.4	10.0	52.7	–	–	41.0	–	[80]
Lublin, Poland	86.4	81.6	–	–	16.1	44.1	–	–	–	241.1	[81]
Çanakkale, Turkey	21	28	12,901	475	21	18	–	–	–	58	[82]
Recife, Brazil	56.5	111.1	–	315.6	12.1	37.4	–	–	29.4	154.4	[83]
Hanoi, Vietnam	3.9	18	271	47	5.31	185	–	–	1.4	1835	[84]
Cuernavaca, Mexico	–	–	4123.5	59.1	84.8	57	–	–	79.5	299.6	[85]
Puebla, Mexico	142.5	109.8	37,800.1	812.9	90.7	36.1	36.8	25.2	104.4	293.2	This study
Volcanic ash											
Puebla, Mexico	62	26.7	–	684.8	46.9	9.2	–	–	79.8	73.4	[63]
Washington, USA	13	32	–	799	15	13	–	–	101	92	[86]
Sicily, Italy	–	106	–	14,200		2	–	–	0.15	160	[87]
Sicily, Italy	0.67	77.4	–	1.9	5.12	13.2	1.0	–	1.1	413	[88]
Baishan, China	0.8	1.0	15,973.0	518.6	0.2	16.2	–	6.76	–	367	[89]
Cumbre Vieja, La Palma Island, Spain	0.07	4.38	533	13.0	0.31	0.61	–	–	1.77	2.02	[90]
Izykh Coalfield, Russia	129	103.0	–	–	290	72.2	0.82	7.41	21.6	387	[91]
Tungurahua, Ecuador	14.5	20.0	10,000.0	120	24.9	10.9	–	–	–	34.1	[92]
Puebla, Mexico	56.3	24.1	32,244.6	788.5	43.8	12.1	14.9	19.5	79.0	137.1	This study

To identify the relationships between elements, Spearman correlation analysis was performed on the data obtained from the dust and ash samples. Street dust samples showed positive and significant correlations in Ni, Cr, Cu, Fe, Mn, Pb and Ti, suggesting that these metals derive from an anthropogenic source; this is in line with previous research suggesting their relation to this type of origin [93]. Meanwhile, Y and Sr showed positive correlations with ash, suggesting the same (natural) origin; on the other hand, Rb presented a negative and significant correlation with Cr, Fe, Mn, Ni, Pb and Ti, from which follows that it also has a natural origin (Figure 3).

The volcanic ash samples presented positive and significant correlations with Sr, Cu, Fe, K, Mn, Rb and Ti. In contrast, negative and significant correlations were observed for Ca with respect to Fe, Ti and Y; Zn with respect to Fe, Rb and Zr; and Cr with respect to Cu (Figure 3), which supports the idea that the volcanic ash was enriched with particles derived from anthropogenic activities; attributed to the city's air pollution, which causes the incorporation of airborne particles into the volcanic ash.

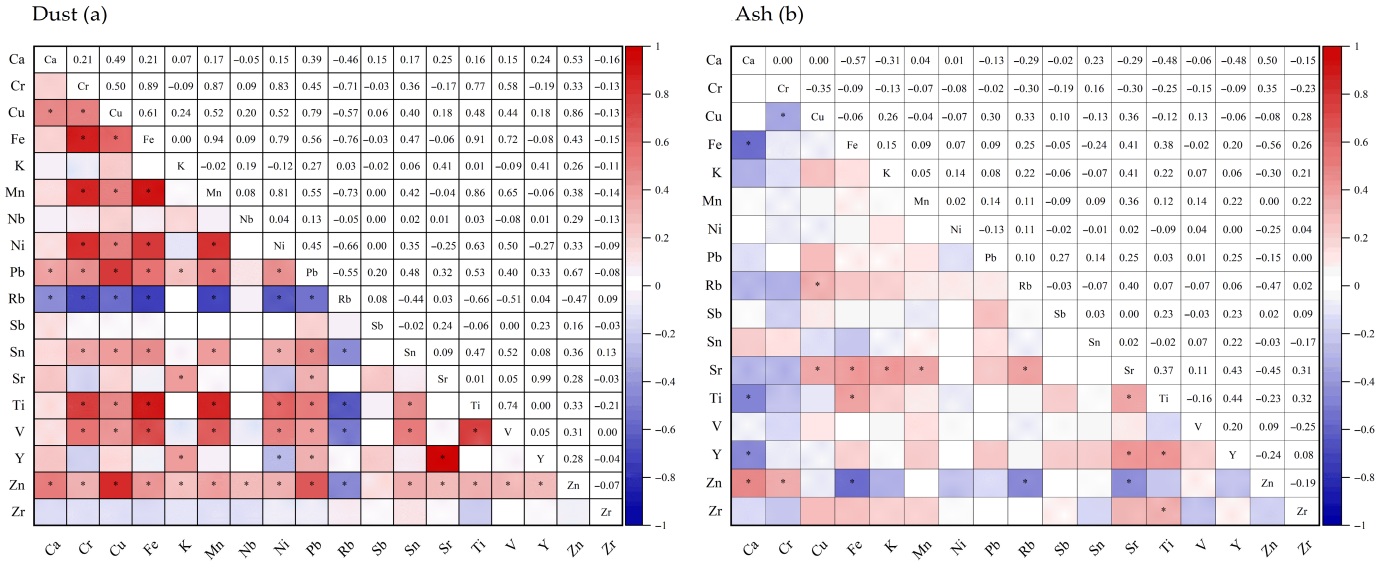


Figure 3. Spearman correlation coefficients between elements in dust (**a**) and ash (**b**) samples. Upper triangle indicates correlation values, the lower triangle indicates the level of correlation; * statistical significance $p \leq 0.05$.

3.2. X-Ray Diffraction and Morphology Analyses

The results indicated that muscovite, albite and stilbite calcium were the main minerals present in the dust and volcanic ash, while mangani-obertiite occurred only in dust samples (Figure 4). It should be noted that muscovite is a mineral for which the adsorption of HMs such as Cu, Zn and Pb has been previously reported [94].

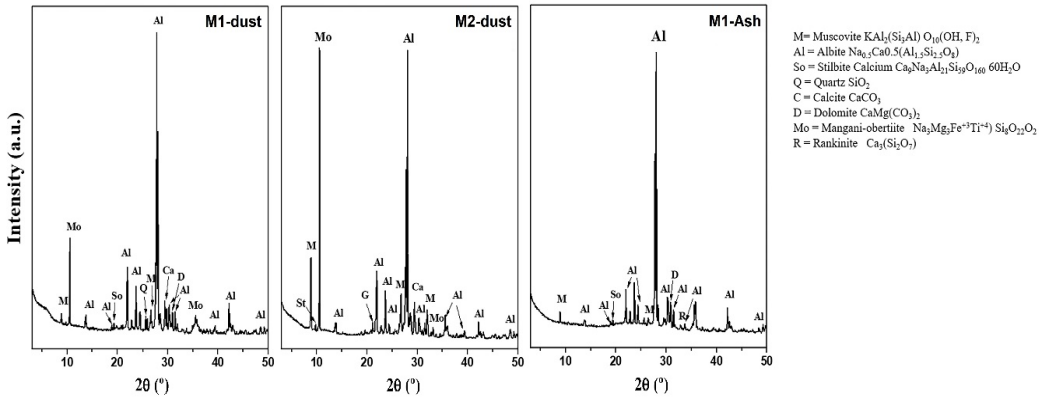


Figure 4. X-ray diffractograms of street dust and volcanic ash samples.

The Sb concentrations could be related to minerals such as Sb_2O_3 and Sb_2S_3, which are used in the production of polyethylene terephthalate—a thermoplastic polymer used in beverage and food containers, as well as textile fibers. They are also used as flame-retardant agents in plastics, and Sb_2S_3 has been introduced into brake pads as a substitute for asbestos [3].

The street dust and volcanic ash particles evaluated via scanning electron microscopy showed laminar and spherical morphologies (Figure 5). Previous studies have concluded that spherical particles come mainly from the combustion of gasoline, while lamellar forms come from the wear of vehicle brakes [95,96]. This suggests that, when the ash is dispersed, it combines with dust particles before deposition.

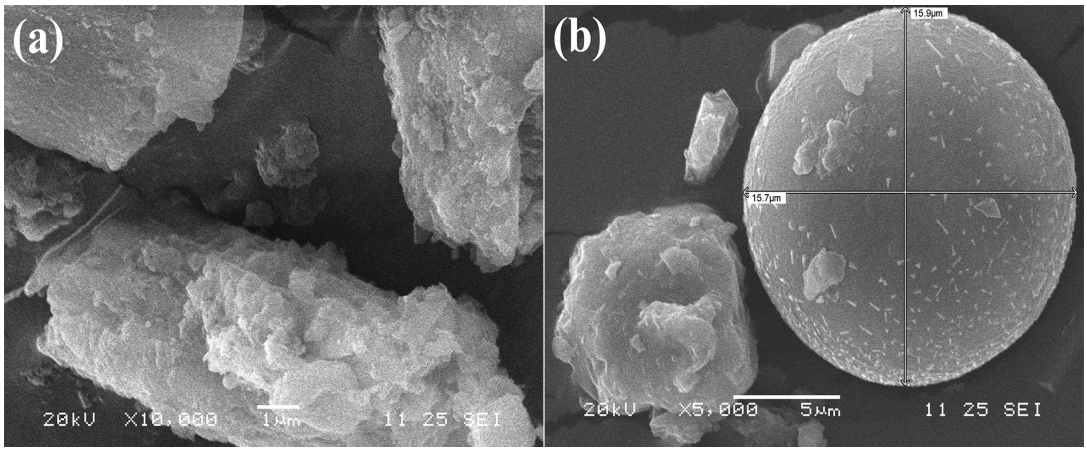


Figure 5. Particles observed by SEM in dust (**a**) and ash (**b**) samples.

3.3. Pollution Levels

3.3.1. Contamination Factor

The average CF values showed higher levels in street dust samples than in volcanic ash samples, except for Rb, Sr and Y, which showed similar averages in both samples. In the street dust samples, Rb, Ti, V and Zr showed a low level of contamination in 100, 98, 73 and 98% of the samples evaluated, respectively; while Cr, Cu, Mn, Ni, Pb, Sr and Y showed moderate contamination in 70, 65, 98, 47, 58, 90 and 100% of samples, respectively; Ni and Zn showed a considerable level of contamination in 53 and 33% of samples, respectively; and Sb, Sn and Zn showed a high level of contamination in 100, 92 and 58% of the samples evaluated, respectively. The high level of Sb contamination can be attributed to the introduction of the mineral Sb_2O_3 into automobile brake pads [3], which has increased its concentrations in the urban area of Puebla. The volcanic ash samples showed low to moderate contamination levels for Cr, Cu, Mn, Ni, Pb, Rb, Sr, Ti, V, Y, Zn and Zr. In contrast, Sb and Sn showed a high contamination level in 100 and 68% of samples, respectively (see Figure 6); this supports the idea of these elements combining with ash when it disperses in urban areas, as Sb and Sn are related to vehicular emissions in cities [3].

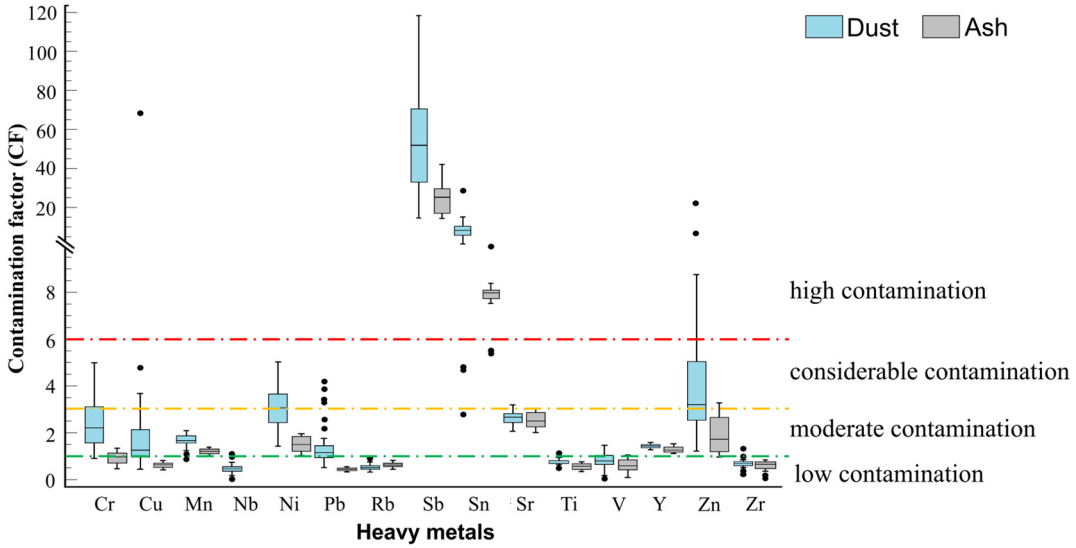


Figure 6. Heavy metal contamination factor values for urban dust and volcanic ash samples.

3.3.2. Geoaccumulation Index

The Igeo values for HMs in street dust samples demonstrated that Cu, Nb, Pb, Rb, Ti, V, Y and Zr were in the uncontaminated category for 70, 100, 80, 100, 100, 100, 87 and 100% of the samples, respectively; Cr and Mn showed contamination levels ranging from uncontaminated to moderately contaminated in 53 and 82% of the samples, respectively; Ni and Zn showed the highest percentages in the levels of uncontaminated to moderately contaminated and moderate contamination, in 45 and 53% and 38 and 47% of the samples, respectively; Sn showed moderate to solid contamination in 67% of the samples, while 23% of the samples showed solid contamination; and Sb showed a level of substantial contamination in 33% of the samples, strong to extreme contamination in 52% of samples, and extreme contamination in 7% of the samples (Figure 6). On the other hand, in the volcanic ash samples, Cr, Cu, Pb, Rb, V, Ti and Zr were in the uncontaminated category in 100% of samples, while that for Y was 93%; Mn and Sr showed a level of uncontaminated to moderate contamination in 100 and 90% of samples, respectively; Ni and Zn showed levels of uncontaminated to moderate contamination and moderate contamination in 50 and 50% and 45 and 43% of samples, respectively; Sn showed moderate and moderate to heavy contamination in 30 and 55% of samples, respectively; and, finally, Sb showed moderate to heavy contamination in 58% and strong to extreme contamination in 40% of the samples (Figure 7).

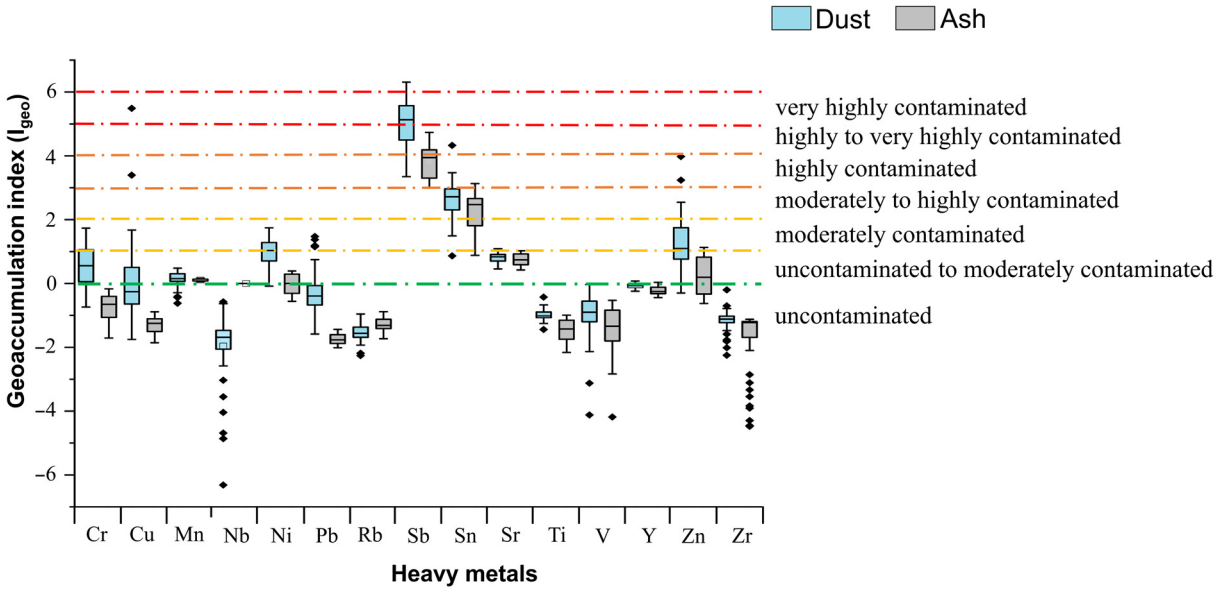


Figure 7. Geoaccumulation index values for heavy metals in urban dust and volcanic ash samples.

3.3.3. Spatial Analysis

The contaminant load index (PLI) was used to evaluate the degree of soil contamination due to the accumulation of HM. For this study, considering those that presented a considerable to high level of contamination according to the CF results, eight elements were chosen.

The PLI values for dust samples ranged from 2.0 to 8.2, while those for ash samples ranged from 1.5 to 2.3, indicating contamination with the elements evaluated and revealing a higher degree of contamination in street dust compared to volcanic ash (Figure 8).

The highest values in dust samples were detected in the northern area of urban Puebla. This can be attributed to the fact that the points that were sampled are located near a highway with high vehicular flow. In particular, when considering the fact that Sb was the element that predominated in the PLI, it is relevant that Puebla is a city characterized by

high vehicular flows, and this element is associated with brake wear [3,64,67]. Furthermore, one sample presented a high concentration of Cu, which may be related to its proximity to an industrial zone and two main highways (Figure 8).

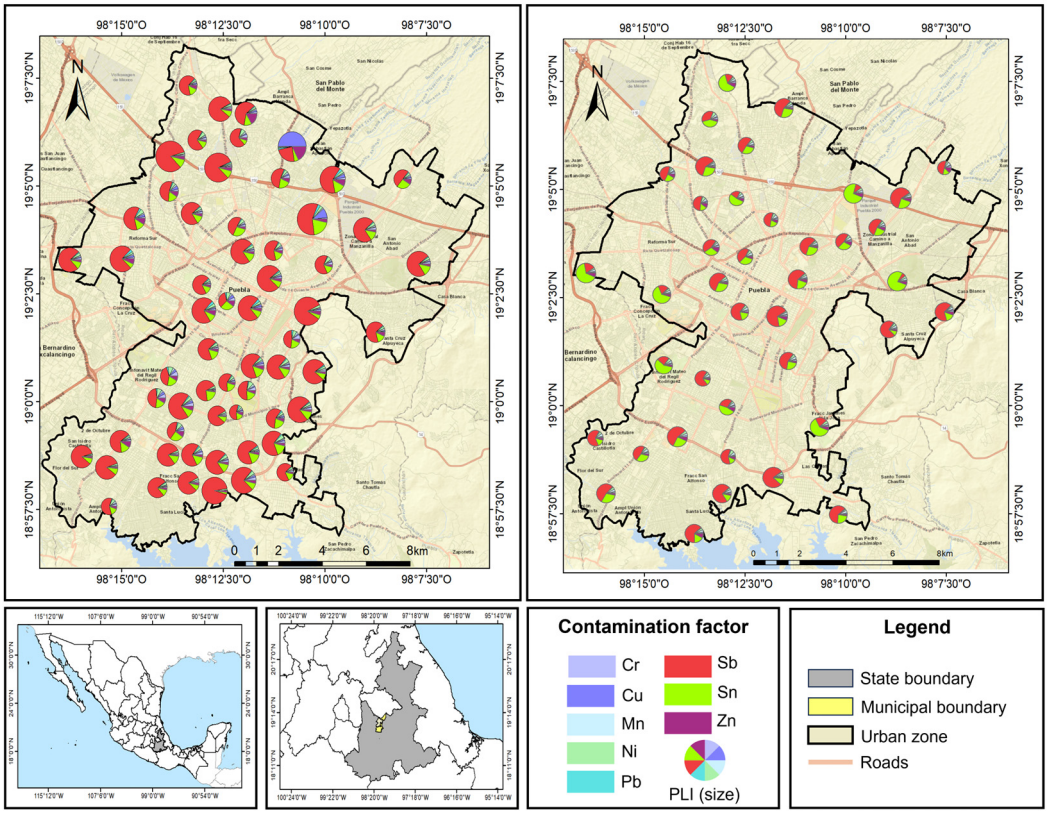


Figure 8. Pollution factor and PLI in urban dust (**left**) and volcanic ash (**right**) samples in the urban area of Puebla.

On the other hand, the PLI values for the volcanic ash samples showed lower values than those detected in dust (Figure 8), with Sn being the predominant element in most of the samples; however, at some sampled locations, Sb predominated. This may be due to the ash combining with urban dust particles at the time that it fell, as these elements showed the highest contamination levels in the CF and Igeo results.

3.4. Risk to Human Health

Regarding human health risks (Figure 9), a non-carcinogenic hazard index (HI) > 1 (red dotted line) was obtained in street dust samples for Cr and Sb with respect to exposure in children. In contrast, Cu, Fe, Mn, Ni, Pb, Sn, V and Zn showed HI values less than 0.25 in most of the dust and ash samples (Figure 9a). For adults, the hazard indices for Cr, Cu, Fe, Mn, Ni, Pb, Sb, Sn, V and Zn in dust and ash samples were all less than 0.1 (green dotted line), except for some dust samples presenting values for Cr and Sb that were close to 0.20 and 0.30, respectively (Figure 9b).

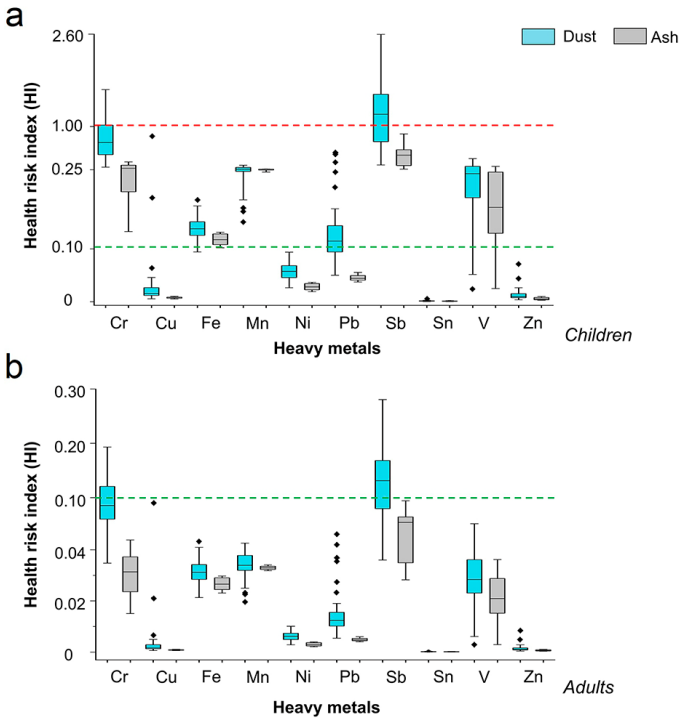


Figure 9. Non-carcinogenic hazard index (HI) for children (**a**) and adults (**b**) regarding urban dust and volcanic ash.

These results demonstrate that the Cr and Sb levels in urban street dust samples pose a health risk to the child population; in particular, exposure to Cr and Sb can cause damage to the cardiovascular and respiratory systems, and may even trigger the development of some cancers [20].

Even though the HIs for children with respect to Mn and Pb in dust samples were generally within the safe limit (<1), caution is still necessary as some of the samples presented high concentrations of these HMs; in particular, prolonged exposure to these HMs can negatively affect human health, potentially triggering neurological, motor and respiratory conditions [22,29,97,98].

Compared to other cities (Table 3), few studies have reported V, Fe and Sb concentrations in urban dust and volcanic ash. In this study, Sb exceeded the limit recommended by the US EPA; in comparison, the city of Düzce, Turkey, came closest to this limit.

Like Puebla, the city of Düzce, Turkey [98] is surrounded by mountains, both of which have tectonic and volcanic origins; this may explain the higher concentrations of Sb in the urban dust of these cities.

On the other hand, Cr, Mn and Pb exceeded the recommended limit (HI > 1) in the cities of Tianshui, Gómez Palacios and Madrid, respectively, with children being the most vulnerable population. Meanwhile, Cu, Fe, Ni, V and Zn have not been reported at concentrations that represent any risk to human health. Regarding the volcanic ash samples, they do not represent a potential risk; however, Cr, Cu, Mn, Sb and V concentrations are close to the risk threshold for the child population in the cities of Puebla and Baishan.

The RI values obtained for Ni and Pb in city dust and volcanic ash samples were similar, with values of 8.79×10^{-8} and 2.10 ± 10^{-9}, respectively. These values are exceeded by established tolerable risk values and, so, the risk of the population developing cancer due to exposure to these HMs is very low [99]. However, Cr presented a value of 6.89×10^{-6}, which represents an elevated risk of contracting some type of cancer in 1 per 10,000 persons due to exposure.

It is urgent to accurately identify the sources of HMs found in high concentrations in street dust, with particular attention to antimony and chromium, considering their high HI values.

More research on urban dust and volcano ash is necessary; in particular, detailed analyses (e.g., involving physical, chemical and mineralogical characterization) of particles of different sizes are essential, mainly respirable particles. It would also be useful to investigate the toxicity of nanoparticles, either in human tissue culture or animal models [100].

Table 3. Comparison of hazard index (HI) values for nine metallic elements in children and adults in different parts of the world.

City		Cr	Cu	Fe	Mn	Ni	Pb	Sb	V	Zn	Reference
Urban dust											
Gómez Palacios, Mexico	Child	–	1.4×10^{-2}	6.8×10^{-2}	1.3	1.8×10^{-2}	2.1×10^{-1}	–	–	4.7×10^{-2}	[29]
	Adult	–	1.5×10^{-3}	1.5×10^{-2}	1.7×10^{-1}	1.9×10^{-3}	2.3×10^{-2}	–	–	5.1×10^{-3}	
Düzce, Turkey	Child	7.9×10^{-2}	1.6×10^{-2}	4.0×10^{-2}	4.1×10^{-2}	1.0×10^{-2}	1.1×10^{-1}	5.2×10^{-1}	5.0×10^{-3}	7.4×10^{-3}	[98]
	Adult	2.3×10^{-2}	2.0×10^{-3}	2.0×10^{-2}	1.1×10^{-2}	1.2×10^{-3}	1.5×10^{-2}	1.5×10^{-1}	2.5×10^{-2}	9.4×10^{-4}	
Dhaka, Bangladesh	Child	9.7×10^{-1}	1.1×10^{-2}	–	8.6×10^{-2}	1.7×10^{-2}	5.4×10^{-2}	–	–	7.6×10^{-3}	[101]
	Adult	2.9×10^{-1}	1.5×10^{-3}	–	2.2×10^{-2}	2.4×10^{-3}	8.6×10^{-3}	–	–	1.1×10^{-3}	
Delhi, India	Child	–	3.7×10^{-4}	4.0×10^{-3}	4.0×10^{-3}	4.7×10^{-4}	3.2×10^{-4}	–	–	2.3×10^{-3}	[102]
	Adult	–	1.8×10^{-3}	2.2×10^{-2}	2.1×10^{-1}	4.6×10^{-3}	1.5×10^{-2}	–	–	1.3×10^{-2}	
Lagos, Nigeria	Child	5.2×10^{-1}	2.0×10^{-2}	1.3×10^{-1}	1.0×10^{-2}	1.0×10^{-2}	7.2×10^{-1}	–	–	7.0×10^{-2}	[103]
	Adult	3.0×10^{-1}	1.0×10^{-2}	3.0×10^{-2}	2.0×10^{-3}	1.0×10^{-2}	2.3×10^{-1}	–	–	7.0×10^{-2}	
Tianshui, China	Child	1.6	8.0×10^{-3}	–	8.4×10^{-2}	7.1×10^{-4}	3.0×10^{-1}	–	5.3×10^{-2}	1.1×10^{-2}	[104]
	Adult	1.4	1.72×10^{-3}	–	2.3×10^{-2}	6.2×10^{-4}	6.3×10^{-2}	–	1.1×10^{-2}	2.3×10^{-5}	
Madrid, Spain	Child	4.3×10^{-1}	1.3×10^{-1}	–	–	2.7×10^{-2}	1.1	–	–	3.8×10^{-2}	[105]
	Adult	4.8×10^{-2}	1.4×10^{-2}	–	–	2.9×10^{-3}	1.1×10^{-1}	–	–	4.1×10^{-3}	
Chiang Mai, Thailand	Child	1.9×10^{-1}	3.3×10^{-2}	–	2.8×10^{-1}	2.5×10^{-2}	2.4×10^{-1}	–	–	2.3×10^{-2}	[106]
	Adult	2.5×10^{-2}	3.9×10^{-3}	–	3.5×10^{-2}	2.9×10^{-3}	2.9×10^{-2}	–	–	2.7×10^{-3}	
Puebla, Mexico	Child	6.9×10^{-1}	3.5×10^{-2}	1.4×10^{-1}	2.6×10^{-1}	5.8×10^{-2}	1.3×10^{-1}	1.20	2.40×10^{-1}	1.3×10^{-2}	This study
	Adult	7.8×10^{-2}	3.8×10^{-3}	3.1×10^{-2}	3.4×10^{-2}	6.3×10^{-3}	1.4×10^{-2}	1.30×10^{-1}	2.80×10^{-2}	1.3×10^{-3}	
Volcanic ash											
Puebla, Mexico	Child	5.5×10^{-2}	1.5×10^{-1}	–	4.1×10^{-2}	5.7×10^{-3}	6.3×10^{-3}	–	–	5.8×10^{-4}	[63]
	Adult	3.9×10^{-2}	2.3×10^{-3}	–	1.8×10^{-2}	3.2×10^{-3}	1.2×10^{-3}	–	–	1.0×10^{-4}	
Baishan, China	Child	1.8×10^{-1}	1.7×10^{-3}	–	1.4×10^{-1}	4.1×10^{-3}	3.9×10^{-2}	–	–	4.8×10^{-3}	[89]
	Adult	3.3×10^{-1}	5.9×10^{-4}	–	2.3×10^{-2}	1.6×10^{-3}	2.6×10^{-2}	–	–	3.9×10^{-3}	
Puebla, Mexico	Child	2.8×10^{-1}	7.3×10^{-3}	1.2×10^{-1}	2.6×10^{-1}	2.7×10^{-2}	4.8×10^{-2}	5.9×10^{-1}	1.9×10^{-1}	5.3×10^{-3}	This study
	Adult	3.1×10^{-2}	7.9×10^{-4}	2.7×10^{-2}	3.3×10^{-2}	2.9×10^{-3}	5.2×10^{-3}	6.4×10^{-2}	2.2×10^{-2}	5.7×10^{-4}	

4. Conclusions

According to the reviewed literature, several similar studies have been conducted in various parts of the world; however, the contribution of this study in the city of Puebla reinforces the fact that each city presents different urbanization dynamics, thus emitting different concentrations of HMs. Therefore, such studies allow us to better understand the pollution levels of different cities, enabling the development of targeted mitigation strategies and, thus, helping to address health risks related to HMs.

This study focused on the current situation of heavy metal contamination in urban dust and volcanic ash in the city of Puebla, highlighting high levels of Cu and Zn contamination in some samples. Furthermore, Sb and Sn presented extreme contamination in most of the urban dust and volcanic ash samples, while Cr, Cu, Ni and Pb showed moderate to considerable contamination levels in most of the samples. The obtained results suggest that these HMs have a similar origin, which is assumed to be anthropogenic and mainly due to vehicular traffic.

The background values used to evaluate HM pollution indices in this study may have limitations due to the presence of nearby volcanic activity—especially considering that, although the activity of Popocatépetl has remained relatively constant, there are periods of inactivity. Therefore, it is recommended that periodic assessments of pollution levels in the city of Puebla be conducted in order to more accurately understand the dynamics of anthropogenic pollutants.

According to the dust/ash ratio values, the concentrations of Cr, Cu, Fe, Mn, Nb, Ni, Pb, Sb, Sn and Zn were higher in street dust, indicating their primary emission sources to be anthropogenic. Meanwhile, the origin of Ca, K, Rb, Sr, Ti, V, Y and Zr may be volcanic. Notably, the V concentrations were above the limits permitted by the Mexican standard, and prolonged exposure could thus represent a health risk.

The non-carcinogenic risk index in the human population due to exposure to heavy metals in the volcanic ash samples did not indicate a considerable risk; this could be attributed to the low concentrations, which may be related to the number of volcanic events and dispersion by the action of the wind. Nevertheless, in the city of Puebla, the urban dust is enriched with metals derived from the volcanic activity.

The antimony (Sb) and chromium (Cr) present in street dust pose a non-carcinogenic risk to children, potentially triggering diseases associated with these elements. Furthermore, chronic exposure to manganese (Mn) and lead (Pb) could lead to various conditions or diseases related to these elements (again, primarily in children).

The carcinogenic index results suggest that Cr monitoring is required to ensure that exposure levels remain within safe limits.

It is recommended that a monitoring system for urban dust and volcanic ash be implemented. In addition, a city cleaning plan should be designed and implemented, considering both environmental matrices. As the indicated health risks are elevated in the child population, environmental and government authorities should take measures to effectively reduce pollution levels.

Supplementary Materials: The following supporting information can be downloaded at https://www.mdpi.com/article/10.3390/environments13030148/s1. Table S1. Interpretation of the Igeo, CF and PLI results; Table S2. Exposure factors for human health risk assessment; Table S3. Reference doses and cancer slope factors for each route of exposure.

Author Contributions: Methodology, writing—original draft: M.S.-M., M.Á.V.-P. and M.G.T.-A.; formal analysis: M.S.-M., F.B. and A.G.; resources: P.Q., F.B. and M.G.T.-A.; writing—original draft: M.S.-M. and M.G.T.-A.; writing—review and editing: M.Á.V.-P., M.G.T.-A., A.G., P.Q. and F.B. All authors have read and agreed to the published version of the manuscript.

Funding: This research received no external funding.

Data Availability Statement: The original contributions presented in this study are included in the article/Supplementary Materials. Further inquiries can be directed to the 2 corresponding authors.

Acknowledgments: We give thanks to the National Laboratory of Nano and Biomaterials (LANNBIO), Cinvestav-IPN, to Patricia Quintana for access to LANNBIO, to M.C. Daniel Aguilar for obtaining the diffractograms, and to Eng. Mario Herrera, Ariel Bagundo, and Daniel Brito for corrective maintenance work on the diffractometer. We also extend our thanks to SECIHTI for awarding a postdoctoral grant to Miguel Santoyo-Martínez (591472) under the program "Becas Posdoctorales por Mexico" in Benemérita Universidad Autónoma de Puebla.

Conflicts of Interest: The authors declare no conflicts of interest.

Abbreviations

Heavy metal (HM), arsenic (As), cadmium (Cd), mercury (Hg), lead (Pb), copper (Cu), Chromium (Cr), manganese (Mn), nickel (Ni), zinc (Zn), X-ray diffraction (XRD), contamination factor (CF), geoaccumulation index (Igeo), pollution load index (PLI), United States Environmental Protection Agency (US EPA), estimated daily intake by ingestion (EDIing), estimated daily intake by inhalation (EDIinh), estimated daily intake by dermal contact (EDIder), reference dose (RfD), hazard quotient (HQ), hazard index (HI), incremental lifetime cancer risk (ILCR), lifetime average daily dose (LADD), cancer slope factor (CSF), calcium (Ca), iron (Fe), potassium (K), niobium (Nb), rubidium

(Rb), antimony (Sb), tin (Sn), strontium (Sr), titanium (Ti), yttrium (Y), vanadium (V), zirconium (Zr), street dust/volcanic ash concentration ratio (D/A).

References

1. Roy, S.; Gupta, S.K.; Prakash, J.; Habib, G.; Kumar, P. A global perspective of the current state of heavy metal contamination in road dust. *Environ. Sci. Pollut. Res.* **2022**, *29*, 33230–33251. [CrossRef] [PubMed]
2. Gupta, V. Vehicle-generated heavy metal pollution in an urban environment and its distribution into various environmental components. In *Environmental Concerns and Sustainable Development*; Shukla, V., Kumar, N., Eds.; Springer: Singapore, 2020; pp. 113–127. [CrossRef]
3. Sager, M. Urban soils and road dust—Civilization effects and metal pollution—A review. *Environments* **2020**, *7*, 98. [CrossRef]
4. Wang, W.; Zhang, J.; Huang, G.; Pryjomska-Ray, I.; Volmer, D.A.; Cai, Z. Tire-additive chemicals and their derivatives in urban road dust: Spatial distributions, exposures, and associations with tire and road wear particles. *J. Hazard. Mater.* **2025**, *490*, 137749. [CrossRef]
5. Singh, R.; Ram, K. Meta-analysis of polyaromatic hydrocarbons in road dust: An emerging threat in urban environment. *Urban Clim.* **2024**, *58*, 102172. [CrossRef]
6. Barone, G.; De Giudici, G.; Gimeno, D.; Lanzafame, G.; Podda, F.; Cannas, C.; Mazzoleni, P. Surface reactivity of Etna volcanic ash and evaluation of health risks. *Sci. Total Environ.* **2021**, *761*, 143248. [CrossRef]
7. Popovych, V.; Gapalo, A. Monitoring of ground forest fire impact on heavy metals content in edafic horizons. *J. Ecol. Eng.* **2021**, *22*, 96–103. [CrossRef]
8. Hama, T.; Ito, H.; Kawagoshi, Y.; Nakamura, K.; Kubota, T. Natural attenuation and remobilization of arsenic in a small river contaminated by the volcanic eruption of Mount Iou in southern Kyushu Island, Japan. *J. Hazard. Mater.* **2023**, *455*, 131576. [CrossRef] [PubMed]
9. Schiavo, B.; Morton-bermea, O.; Meza-Figueroa, D.; Angulo-Molina, A.; Inguaggiato, C.; García-Martínez, R. Mercury concentrations in volcanic ash from the 2023 eruption of popocatépetl volcano (Mexico): Environmental contamination and health risk assessment. *J. South Am. Earth Sci.* **2025**, *167*, 105766. [CrossRef]
10. Francisco, R.R.; Santos, N.E.; Teixeira, L.S.; Korn, M.G.A.; Kolling, L.; Dessuy, M.B.; Araujo, R.G. Determination of mercury in urban dust: Direct sample analysis and establishment of a geochemical baseline. *Talanta Open* **2026**, *13*, 100599. [CrossRef]
11. Isinkaralar, K.; Świsłowski, P.; Isinkaralar, O.; Rajfur, M.; Nguyen, T.N.T.; Di Palma, A.; Gautam, S. Assessing heavy metal pollution in urban children's playgrounds: Comparative analysis of soil, dust, and moss bioaccumulation. *J. Environ. Sci.* **2026**, *160*, 700–712. [CrossRef]
12. Chirino, Y.I.; Sánchez-Pérez, Y.; Osornio-Vargas, Á.R.; Rosas, I.; García-Cuellar, C.M. Sampling and composition of airborne particulate matter (PM10) from two locations of Mexico City. *Data Brief* **2015**, *4*, 353–356. [CrossRef]
13. García-Rico, L.; Meza-Figueroa, D.; Gandolfi, A.J.; Del Río-Salas, R.; Romero, F.M.; Meza-Montenegro, M.M. Dust–metal sources in an urbanized arid zone: Implications for health-risk assessments. *Arch. Environ. Contam. Toxicol.* **2016**, *70*, 522–533. [CrossRef]
14. Men, C.; Liu, R.; Xu, F.; Wang, Q.; Guo, L.; Shen, Z. Pollution characteristics, risk assessment, and source apportionment of heavy metals in road dust in Beijing, China. *Sci. Total Environ.* **2018**, *612*, 138–147. [CrossRef]
15. Yu, S.; Zhu, Y.G.; Li, X.D. Trace metal contamination in urban soils of China. *Sci. Total Environ.* **2012**, *421*, 17–30. [CrossRef]
16. Hwang, H.M.; Fiala, M.J.; Park, D.; Wade, T.L. Review of pollutants in urban road dust and stormwater runoff: Part 1. Heavy metals released from vehicles. *Int. J. Urban Sci.* **2016**, *20*, 334–360. [CrossRef]
17. Chen, G.; Wang, Y.; Li, S.; Cao, W.; Ren, H.; Knibbs, L.D.; Guo, Y. Spatiotemporal patterns of PM10 concentrations over China during 2005–2016: A satellite-based estimation using the random forests approach. *Environ. Pollut.* **2018**, *242*, 605–613. [CrossRef]
18. Ferreira-Baptista, L.; De Miguel, E. Geochemistry and risk assessment of street dust in Luanda, Angola: A tropical urban environment. *Atmos. Environ.* **2005**, *39*, 4501–4512. [CrossRef]
19. Wei, B.; Yang, L. A review of heavy metal contaminations in urban soils, urban road dusts and agricultural soils from China. *Microchem. J.* **2010**, *94*, 99–107. [CrossRef]
20. Tchounwou, P.B.; Yedjou, C.G.; Patlolla, A.K.; Sutton, D.J. Heavy Metal Toxicity and the Environment. In *Molecular, Clinical and Environmental Toxicology*; Luch, A., Ed.; Springer: Basel, Switzerland, 2012; Volume 101, pp. 133–164. [CrossRef]
21. Jan, A.T.; Azam, M.; Siddiqui, K.; Ali, A.; Choi, I.; Haq, Q.M.R. Heavy metals and human health: Mechanistic insight into toxicity and counter defense system of antioxidants. *Int. J. Mol. Sci.* **2015**, *16*, 29592–29630. [CrossRef] [PubMed]
22. Kong, S.; Lu, B.; Bai, Z.; Zhao, X.; Chen, L.; Han, B.; Jiang, H. Potential threat of heavy metals in re-suspended dusts on building surfaces in oilfield city. *Atmos. Environ.* **2011**, *45*, 4192–4204. [CrossRef]
23. Williams, M.; Todd, G.D.; Roney, N.; Crawford, J.; Coles McClure, P.R.; Garey, J.D.; Zaccaria, K.; Citra, M. Toxicological Profile for Manganese. U.S. Department Of Health And Human Services. Public Health Service 2012. Available online: https://www.ncbi.nlm.nih.gov/books/NBK158872/ (accessed on 27 January 2026).

24. Mohmand, J.; Eqani, S.A.M.A.S.; Fasola, M.; Alamdar, A.; Mustafa, I.; Ali, N.; Liu, L.; Peng, S.; Shen, H. Human exposure to toxic metals via contaminated dust: Bioaccumulation trends and their potential risk estimation. *Chemosphere* **2015**, *132*, 142–151. [CrossRef]
25. Yadav, I.C.; Devi, N.L.; Singh, V.K.; Li, J.; Zhang, G. Spatial distribution, source analysis, and health risk assessment of heavy metals contamination in house dust and surface soil from four major cities of Nepal. *Chemosphere* **2019**, *218*, 1100–1113. [CrossRef]
26. Delibašić, Š.; Đokić-Kahvedžić, N.; Karić, M.; Keskin, I.; Velispahić, A.; Huremović, J.; Pašalić, A. Health risk assessment of heavy metal contamination in street dust of Federation of Bosnia and Herzegovina. Human and Ecological Risk Assessment. *Int. J.* **2020**, *27*, 1296–1308. [CrossRef]
27. Aguilera, A.; Bautista-Hernández, D.; Bautista, F.; Goguitchaichvili, A.; Cejudo, R. Is the Urban Form a Driver of Heavy Metal Pollution in Road Dust? Evidence from Mexico City. *Atmosphere* **2020**, *12*, 266. [CrossRef]
28. Bai, W.; Zhao, X.; Yin, B.; Guo, L.; Zhang, W.; Wang, X.; Yang, W. Characteristics of PM2. 5 in an industrial city of Northern China: Mass concentrations, chemical composition, source apportionment, and health risk assessment. *Int. J. Environ. Res. Public Health* **2022**, *19*, 5443. [CrossRef]
29. Santoyo-Martínez, M.; Aguilera, A.; Gallegos, Á.; Puente, C.; Goguitchaichvili, A.; Bautista, F. Pollution Levels and Potential Health Risks of Potentially Toxic Elements in Indoor and Outdoor Dust during the COVID-19 Era in Gómez Palacios City, Mexico. *Land* **2022**, *12*, 29. [CrossRef]
30. Saleem, M.; Sens, D.A.; Somji, S.; Pierce, D.; Wang, Y.; Leopold, A.; Garrett, S.H. Contamination assessment and potential human health risks of heavy metals in urban soils from Grand Forks, North Dakota, USA. *Toxics* **2023**, *11*, 132. [CrossRef] [PubMed]
31. Wijesiri, B.; Egodawatta, P.; McGree, J.; Goonetilleke, A. Process variability of pollutant build-up on urban road surfaces. *Sci. Total Environ.* **2015**, *518–519*, 434–440. [CrossRef] [PubMed]
32. Ihl, T.; Bautista, F.; Cejudo, R.; Delgado, C.; Goguichaishvili, A.; Quitana, P.; Aguilar, D. Concentration of toxic elements in topsoils of the Metropolitan area of Mexico City: A spatial analysis using Ordinary Kriging and Indicator Kriging. *Rev. Int. Contam. Ambie.* **2015**, *31*, 47–62. Available online: https://www.scielo.org.mx/scielo.php?script=sci_arttext&pid=S0188-49992015000100004 (accessed on 27 January 2026).
33. Cortés, J.L.; Bautista, F.; Delgado, C.; Quintana, P.; Aguilar, D.; García, A.; Figuero, C.; Gogichaishvili, A. Distribución espacial de los metales pesados en polvos urbanos de la ciudad de Ensenada, Baja California, México. *Rev. Chapingo Ser. Cienc. For. Y Del Ambiente* **2017**, *23*, 47–60. [CrossRef]
34. Andrade, A.; Aguilera, A.; Gallegos, Á.; Aguilar, Y.; Quintana, P.; Bautista, F. Heavy metals in urban dust inside and outside homes during the COVID-19 pandemic in Mérida, Yucatán, México. *Air Qual. Atmos. Health* **2023**, *16*, 2337–2349. [CrossRef]
35. Bautista-Hernández, D.A.; Bautista, F.; Goguitchaichvili, A.; Cejudo, R. Street dust pollution by heavy metals: A geographically weighted regression approach in México City. *Int. J. Environ. Sci. Technol.* **2023**, *20*, 9795–9822. [CrossRef]
36. Aguilera, A.; Gallegos, Á.; Luna, V.; Hernández, L.; Gutiérrez, M.; Amaro, D.; Bautista, F. Higher heavy metal contamination indoors than outdoors during COVID-19 in Mexico City. *Environ. Sci. Pollut. Res.* **2024**, *31*, 16696–16709. [CrossRef]
37. Chen, H.; Lu, X.; Li, L.Y.; Gao, T.; Chang, Y. Metal contamination in campus dust of Xi'an, China: A study based on multivariate statistics and spatial distribution. *Sci. Total Environ.* **2014**, *484*, 27–35. [CrossRef]
38. Shi, T.; Wang, Y. Metales pesados en el polvo interior: Distribución espacial, factores influyentes y posibles riesgos para la salud. *Sci. Total Environ.* **2021**, *755*, 142367. [CrossRef]
39. Wiseman, C.L.; Levesque, C.; Rasmussen, P.E. Characterizing the sources, concentrations, and resuspension potential of metals and metalloids in the thoracic fraction of urban road dust. *Sci. Total Environ.* **2021**, *786*, 147467. [CrossRef]
40. Madadi, R.; Mohamadi, S.; Rastegari, M.; Karbassi, A.; Rakib, M.R.J.; Khandaker, M.U.; Idris, A.M. Health risk assessment and source apportionment of potentially toxic metal (loid) s in windowsill dust of a rapidly growing urban settlement, Iran. *Sci. Rep.* **2022**, *12*, 19736. [CrossRef]
41. Soto-Jiménez, M.F.; Flegal, A.R. Polvo doméstico contaminado con metales en interiores y exteriores de una zona de fundición vecinal en Torreón, México. *Procedia Environ. Sci.* **2011**, *4*, 134–137. [CrossRef]
42. Ibañez del Rivero, C. Estudio Geoquímico y Morfológico del Polvo Urbano en la Ciudad de Hermosillo, Sonora, México para Identificar Geogénicas y/o Antropogénicas. Master's Thesis, Universidad de Sonora, Hermosillo, Mexico, 2017.
43. Valdez-Cerda, E.; Hinojosa-Reyes, L.; Alfaro-Barbosa, J.M.; Elizondo-Martinez, P.; Acuña-Askar, K. Contamination and chemical fractionation of heavy metals in street dust from the Metropolitan Area of Monterrey, Mexico. *Environ. Sci. Technol.* **2011**, *32*, 1163–1172. [CrossRef] [PubMed]
44. Instituto Nacional De Estadística y Geografía (INEGI). 2024. Available online: www.inegi.gob.mx (accessed on 27 October 2025).
45. Global Volcanism Program Report on Popocatepetl (Mexico). In *Weekly Volcanic Activity Report, 22 November–28 November 2017*; Sennert, S.K., Ed.; Smithsonian Institution and US Geological Survey. Available online: https://volcano.si.edu/reports_weekly.cfm (accessed on 27 October 2025).
46. Martin-Del Pozzo, A.L.; Nieto-Torres, A. Ashfall characteristics and development of the ash monitoring network during three decades of the long-lived eruption of Popocatépetl Volcano, México. *J. Volcanol. Geoth. Res.* **2024**, *454*, 108176. [CrossRef]

47. GEMAS Project Team. *Comisión Nacional para el Conocimiento y Uso de la Biodiversidad (CONABIO) y Secretaría de Recursos Naturales y Medio Ambiente de Durango (SRNYMA). La Biodiversidad en Durango. Estudio de Estado*; CONABIO: Mexico City, México, 2017. Available online: https://www.biodiversidad.gob.mx/region/EEB/estudios/ee_durango (accessed on 2 March 2026).
48. Lozano, R.; Bernal, J.P. Characterization of a new set of eight geochemical reference materials for XRF major and trace element analysis. *Rev. Mex. Cien. Geol.* **2005**, *22*, 329–344. Available online: https://www.rmcg.unam.mx/index.php/rmcg/article/view/841 (accessed on 2 March 2026).
49. Deng, Y.; White, G.N.; Dixon, J.B. *Soil Mineralogy Laboratory Manual*, 12th ed.; Department of Soil and Crop Sciences, Texas A&M University: College Station, TX, USA, 2010; Volume 77, pp. 843–2474.
50. Hakanson, L. An ecological risk index for aquatic pollution control. A sedimentological approach. *Water Res.* **1980**, *14*, 975–1001. [CrossRef]
51. Muller, G. Index of geoaccumulation in sediments of the Rhine River. *GeoJournal* **1969**, *2*, 108–118. Available online: https://www.scirp.org/reference/ReferencesPapers?ReferenceID=1803049 (accessed on 2 March 2026).
52. Varol, M. Assessment of heavy metal contamination in sediments of the Tigris River (Turkey) using pollution indices and multivariate statistical techniques. *J. Hazard. Mater.* **2011**, *195*, 355–364. [CrossRef]
53. Kabata-Pendias, A. *Trace Elements in Soils and Plants*, 4th ed.; CRC Press: Boca Raton, FL, USA; Taylor and Francis Group, LLC: New York, NY, USA, 2011.
54. USEPA Risk Assessment Guidance for Superfund (RAGS) Volume III—Part A: Process for Conducting Probabilistic Risk Assessment, Appendix B. Vol. III. U.S. Environmental Protection Agency, EPA. 2001, 540-R-02–002. Available online: https://www.epa.gov/sites/default/files/2015-09/documents/rags3adt_complete.pdf (accessed on 2 March 2026).
55. Li, X.; Poon, C.-S.; Liu, P.S. Heavy metal contamination of urban soils and street dusts in Hong Kong. *Appl. Geochem.* **2001**, *16*, 1361–1368. [CrossRef]
56. Ali, M.U.; Liu, G.; Yousaf, B.; Abbas, Q.; Ullah, H.; Munir, M.A.M.; Fu, B. Pollution characteristics and human health risks of potentially (eco) toxic elements (PTEs) in road dust from the metropolitan area of Hefei, China. *Chemosphere* **2017**, *181*, 111–121. [CrossRef] [PubMed]
57. Zheng, N.; Liu, J.; Wang, Q.; Liang, Z. Health risk assessment of arsenic exposure to street dust in the zinc smelting district, Northeast China. *Sci. Total Environ.* **2010**, *408*, 726–733. [CrossRef]
58. USEPA Risk Assessment Guidance for Superfund (RAGS). *Volume I. Human Health Evaluation Manual (HHEM). Part E. Supplemental Guidance for Dermal Risk Assessment*; U.S. Environmental Protection Agency, EPA: Washington, DC, USA, 1989; Volume 540, p. 1-89/002. Available online: https://www.epa.gov/risk/risk-assessment-guidance-superfund-rags-part-e (accessed on 2 March 2026).
59. Kurt-Karakus, P.B. Determination of heavy metals in indoor dust from Istanbul, Turkey: Estimation of the health risk. *Environ. Int.* **2012**, *50*, 47–55. [CrossRef] [PubMed]
60. Origin Pro OriginLab Corporation, Northampton, 2023, MA, EE. UU. Available online: https://www.originlab.com/ (accessed on 20 December 2023).
61. Zar, J.H. *Análisis Bioestadístico*, 4th ed.; Pearson Prentice Hall: Upper Saddle River, NJ, USA, 1999; ISBN 0130823902.
62. Alekseenko, V.; Alekseenko, A. The abundance of chemical elements in urban soils. *J. Geochem. Explor.* **2014**, *147*, 245–249. [CrossRef]
63. Shruti, V.C.; Rodríguez-Espinosa, P.F.; Martinez-Tavera, E.; Hernández-Gonzalez, D. Metal concentrations in recent ash fall of Popocatepetl volcano 2016, Central Mexico: Is human health at risk? *Ecotoxicol. Environ. Saf.* **2018**, *162*, 324–333. [CrossRef] [PubMed]
64. Rodríguez-Seijo, A.; Andrade, M.L.; Vega, F.A. Origin and spatial distribution of metals in urban soils. *J. Soils Sediments* **2017**, *17*, 1514–1526. [CrossRef]
65. Schulz, K.J.; Piatak, N.M.; Papp, J.F. *Niobium and Tantalum*; Schulz, K.J., DeYoung, J.H., Jr., Seal, R.R., II, Bradley, D.C., Eds.; Critical Mineral Resources of the United States—Economic and Environmental Geology and Prospects for Future Supply; U.S. Geological Survey Professional Paper; U.S. Geological Survey: Reston, VA, USA, 2017; Volume 1802. [CrossRef]
66. Zhou, L.; Liu, G.; Shen, M.; Liu, Y. Posibles riesgos ecológicos y para la salud de los metales pesados presentes en el polvo interior y exterior en Hefei, China Central. *Chemosphere* **2022**, *302*, 134864. [CrossRef]
67. Grigoratos, T.; Martini, G. Brake wear particle emissions: A review. *Environ. Sci. Pollut. Res.* **2015**, *22*, 2491–2504. [CrossRef]
68. Ondráček, J.; Schwarz, J.; Ždímal, V.; Andělová, L.; Vodička, P.; Bízek, V.; Smolík, J. Contribution of the road traffic to air pollution in the Prague city (busy speedway and suburban crossroads). *Atmos Environ.* **2011**, *45*, 5090–5100. [CrossRef]
69. Fujiwara, F.; Rebagliati, R.J.; Dawidowski, L.; Gómez, D.; Polla, G.; Pereyra, V.; Smichowski, P. Spatial and chemical patterns of size fractionated road dust collected in a megacitiy. *Atmos Environ.* **2011**, *45*, 1497–1505. [CrossRef]
70. Horváth, A.; Szűcs, P.; Bidló, A. Soil condition and pollution in urban soils: Evaluation of the soil quality in a Hungarian town. *J. Soils Sediments* **2015**, *15*, 1825–1835. [CrossRef]

71. Scheib, A.J.; Flight, D.M.A.; Birke, M.; Tarvainen, T.; Locutura, J.; GEMAS Project Team. The geochemistry of niobium and its distribution and relative mobility in agricultural soils of Europe. *Geochem. Explor. Environ. Anal.* **2012**, *12*, 293–302. [CrossRef]
72. Secretaría de Medio Ambiente y Recursos Naturales (SEMARNAT) Norma Oficial Mexicana NOM-147-SEMARNAT/SSA1-2004. *Que Establece Criterios para Determinar las Concentraciones de Remediación de Suelos Contaminados por Arsénico, Berilio, Cadmio, Cromo Hexavalente, Mercurio, Níquel, Plomo, Selenio, Talio y Vanadio*; Diario Oficial de la Federación: Mexico City, México, 2007. Available online: https://www.gob.mx/profepa/documentos/norma-oficial-mexicana-nom-147-semarnat-ssa1-2004 (accessed on 27 January 2026).
73. Rodríguez-Mercado, J.J.; Altamirano-Lozano, M.A. Vanadio: Contaminación, metabolismo y genotoxicidad. *Rev. Int. Contam. Ambie.* **2006**, *22*, 173–189.
74. Delgado, C.; Bautista, F.; Gogichaishvili, A.; Cortés, J.L.; Quintana, P.; Aguilar, D.; Cejudo, R. Identificación de las zonas contaminadas con metales pesados en el polvo urbano de la Ciudad de México. *Rev. Int. Contam. Ambient.* **2019**, *35*, 81–100. Available online: https://www.redalyc.org/journal/370/37060163008/html/ (accessed on 2 March 2026). [CrossRef]
75. Rojas-Lemus, M.; López-Valdez, N.; Bizarro-Nevares, P.; González-Villalva, A.; Fortoul, T.I. Vanadio: Exposición atmosférica, efectos en la salud y normatividad en México: Revisión de la literatura. *Rev. Int. Contam. Ambient.* **2024**, *40*, 181–191. [CrossRef]
76. Rasmussen, P.E.; Subramanian, K.S.; Jessiman, B.J. A multi-element profile of house dust in relation to exterior dust and soils in the city of Ottawa, Canada. *Sci. Total Environ.* **2001**, *267*, 125–140. [CrossRef]
77. Varrica, D.; Dongarra, G.; Sabatino, G.; Monna, F. Inorganic geochemistry of roadway dust from the metropolitan area of Palermo, Italy. *Environ. Geol.* **2003**, *44*, 222–230. [CrossRef]
78. Keshavarzi, B.; Tazarvi, Z.; Rajabzadeh, M.A.; Najmeddin, A. Chemical speciation, human health risk assessment and pollution level of selected heavy metals in urban street dust of Shiraz, Iran. *Atmos. Environ.* **2015**, *119*, 1–10. [CrossRef]
79. Meza-Figueroa, D.; González-Grijalva, B.; Del Río-Salas, R.; Coimbra, R.; Ochoa-Landin, L.; Moreno-Rodríguez, V. Señales de tráfico en polvo en suspensión a nivel de peatones en zonas semiáridas: Implicaciones para la exposición humana. *Atmos. Environ.* **2016**, *138*, 4–14. [CrossRef]
80. Al-Madanat, O.; Jiries, A.; Batarseh, M.; Al-Nasir, F. Indoor and outdoor pollution with heavy metals in Al-Karak City, Jordan. *J. Int. Environ. Appl. Sci.* **2017**, *12*, 131–139.
81. Zgłobicki, W.; Telecka, M.; Skupiński, S. Assessment of heavy metal contamination levels of street dust in the city of Lublin, E Poland. *Environ. Earth Sci.* **2018**, *77*, 774. [CrossRef]
82. Parlak, M.; Tunçay, T.; Botsou, F. Heavy metals in soil and sand from playgrounds of Çanakkale city (Turkey), and related health risks for children. *Sustainability* **2022**, *14*, 1145. [CrossRef]
83. Lima, L.H.V.; do Nascimento, C.W.A.; da Silva, F.B.V.; Araújo, P.R.M. Baseline concentrations, source apportionment, and probabilistic risk assessment of heavy metals in urban street dust in Northeast Brazil. *Sci. Total Environ.* **2023**, *858*, 159750. [CrossRef]
84. Makkonen, U.; Vestenius, M.; Huy, L.N.; Anh, N.T.N.; Linh, P.T.V.; Thuy, P.T.; Oanh, N.K. Chemical composition and potential sources of PM2. 5 in Hanoi. *Atmos. Environ.* **2023**, *299*, 119650. [CrossRef]
85. Brito-Hernández, A.; Saldarriaga-Noreña, H.; Rosales-Rivera, M.; García-Betancourt, M.L.; Murillo-Tovar, M.A.; Romero-Aguilar, M.; Figueroa-Lara, J.D.J. Risk Estimation of Heavy Metals Associated with PM2. 5 in the Urban Area of Cuernavaca, México. *Atmosphere* **2024**, *15*, 409. [CrossRef]
86. Taylor, H.E.; Lichte, F.E. Chemical composition of Mount St. Helens volcanic ash. *Geophys. Res. Lett.* **1980**, *7*, 949–952. [CrossRef]
87. Toscano, G.; Caristi, C.; Cimino, G. Sorption of heavy metal from aqueous solution by volcanic ash. *Comptes Rendus. Chimie* **2008**, *11*, 765–771. [CrossRef]
88. Varrica, D.; Tamburo, E.; Dongarrà, G.; Sposito, F. Trace elements in scalp hair of children chronically exposed to volcanic activity (Mt. Etna, Italy). *Sci. Total Environ.* **2014**, *470*, 117–126. [CrossRef]
89. Ma, Q.; Han, L.; Zhang, J.; Zhang, Y.; Lang, Q.; Li, F.; Alu, S. Environmental risk assessment of metals in the volcanic soil of Changbai Mountain. *Int. J. Environ. Res. Public Health* **2019**, *16*, 2047. [CrossRef]
90. Ruggieri, F.; Forte, G.; Bocca, B.; Casentini, B.; Bruna Petrangeli, A.; Salatino, A.; Gimeno, D. Potentially harmful elements released by volcanic ash of the 2021 Tajogaite eruption (Cumbre Vieja, La Palma Island, Spain): Implications for human health. *Sci. Total Environ.* **2023**, *905*, 167103. [CrossRef] [PubMed]
91. Vergunov, A.; Arbuzov, S.; Spears, D.; Kholodov, A.; Ilenok, S. Mineralogy and geochemistry of rare metal (Zr-Nb-Hf-Ta-REE-Ga) coals of the seam XXX of the Izykh Coalfield, Minusinsk Basin, Russia: Implications for more widespread rare metal mineralization in North Asia. *Intl. J. Coal Geol.* **2024**, *289*, 104542. [CrossRef]
92. Carrera-Beltrán, L.; Gavilanes-Terán, I.; Idrovo-Novillo, J.; Valverde, V.H.; Rodríguez-Pinos, A.; Paredes, C.; Signes-Pastor, A.J.; Carbonell-Barrachina, Á.A. Environmental pollution by heavy metals within the area influenced by the Tungurahua volcano eruption-Ecuador. *Ecotoxicol. Environ. Saf.* **2024**, *270*, 115919. [CrossRef]

93. Daher, N.; Saliba, N.A.; Shihadeh, A.L.; Jaafar, M.; Baalbaki, R.; Shafer, M.M.; Sioutas, C. Oxidative potential and chemical speciation of size-resolved particulate matter (PM) at near-freeway and urban background sites in the greater Beirut area. *Sci. Total Environ.* **2014**, *470*, 417–426. [CrossRef]
94. Gier, S.; Johns, W.D. Heavy metal-adsorption on micas and clay minerals studied by X-ray photoelectron spectroscopy. *Appl. Clay Sci.* **2000**, *16*, 289–299. [CrossRef]
95. Aguilera, A.; Morales, J.J.; Goguitchaichvili, A.; García-Oliva, F.; Armendariz-Arnez, C.; Quintana, P.; Bautista, F. Spatial distribution of magnetic material in urban road dust classified by land use and type of road in San Luis Potosí, Mexico. *Air Qual. Atmos. Health* **2020**, *13*, 951–963. [CrossRef]
96. Aguilar, Y.; Bautista, F.; Quintana, P.; Aguilar, D.; Trejo-Tzab, R.; Goguitchaichvili, A.; Chan-Te, R. Color as a new proxy technique for the identification of road dust samples contaminated with potentially toxic elements: The case of Mérida, Yucatán, México. *Atmosphere* **2021**, *12*, 483. [CrossRef]
97. Jadoon, W.A.; Khpalwak, W.; Chidya, R.C.G.; Abdel-Dayem, S.M.M.A.; Takeda, K.; Makhdoom, M.A.; Sakugawa, H. Evaluation of levels, sources and health hazards of road-dust associated toxic metals in Jalalabad and Kabul Cities, Afghanistan. *Arch. Environ. Contam. Toxicol.* **2018**, *74*, 32–45. [CrossRef] [PubMed]
98. Taşpınar, F.; Bozkurt, Z. Heavy metal pollution and health risk assessment of road dust on selected highways in Düzce, Turkey. *Environ. Forensics* **2018**, *19*, 298–314. [CrossRef]
99. Lu, X.; Wu, X.; Wang, Y.; Chen, H.; Gao, P.; Fu, Y. Risk assessment of toxic metals in street dust from a medium-sized industrial city of China. *Ecotoxicol. Environ. Saf.* **2014**, *106*, 154–163. [CrossRef] [PubMed]
100. Hammond, J.; Maher, B.A.; Gonet, T.; Bautista, F.; Allsop, D. Oxidative Stress, Cytotoxic and Inflammatory Effects of Urban Ultrafine Road-Deposited Dust from the UK and Mexico in Human Epithelial Lung (Calu-3) Cells. *Antioxidants* **2022**, *11*, 1814. [CrossRef]
101. Rahman, M.S.; Khan, M.D.H.; Jolly, Y.N.; Kabir, J.; Akter, S.; Salam, A. Assessing risk to human health for heavy metal contamination through street dust in the Southeast Asian Megacity: Dhaka, Bangladesh. *Sci. Total Environ.* **2019**, *660*, 1610–1622. [CrossRef]
102. Siddiqui, Z.; Khillare, P.S.; Jyethi, D.S.; Aithani, D.; Yadav, A.K. Pollution characteristics and human health risk from trace metals in roadside soil and road dust around major urban parks in Delhi city. *Air Qual. Atmos. Health* **2020**, *13*, 1271–1286. [CrossRef]
103. Taiwo, A.M.; Musa, M.O.; Oguntoke, O.; Afolabi, T.A.; Sadiq, A.Y.; Akanji, M.A.; Shehu, M.R. Spatial distribution, pollution index, receptor modelling and health risk assessment of metals in road dust from Lagos metropolis, Southwestern Nigeria. *Environ. Adv.* **2020**, *2*, 100012. [CrossRef]
104. Tan, B.; Wang, H.; Wang, X.; Ma, C.; Zhou, J.; Dai, X. Health risks and source analysis of heavy metal pollution from dust in Tianshui, China. *Minerals* **2021**, *11*, 502. [CrossRef]
105. Delgado-Iniesta, M.J.; Marín-Sanleandro, P.; Díaz-Pereira, E.; Bautista, F.; Romero-Muñoz, M.; Sánchez-Navarro, A. Estimation of ecological and human health risks posed by heavy metals in street dust of Madrid City (Spain). *Int. J. Environ. Res. Public Health* **2022**, *19*, 5263. [CrossRef] [PubMed]
106. Somsunun, K.; Prapamontol, T.; Kuanpan, T.; Santijitpakdee, T.; Kohsuwan, K.; Jeytawan, N.; Thongjan, N. Health Risk Assessment of Heavy Metals in Indoor Household Dust in Urban and Rural Areas of Chiang Mai and Lamphun Provinces, Thailand. *Toxics* **2023**, *11*, 1018. [CrossRef] [PubMed]

Disclaimer/Publisher's Note: The statements, opinions and data contained in all publications are solely those of the individual author(s) and contributor(s) and not of MDPI and/or the editor(s). MDPI and/or the editor(s) disclaim responsibility for any injury to people or property resulting from any ideas, methods, instructions or products referred to in the content.